

Enhanced diagrams: re-summation of unitarity cuts

S. Ostapchenko

Forschungszentrum Karlsruhe, Institut für Kernphysik, 76021 Karlsruhe, Germany

D. V. Skobeltsyn Institute of Nuclear Physics, Moscow State University, 119992 Moscow, Russia

February 8, 2020

Abstract

Unitarity cuts of enhanced pomeron diagrams are analyzed in the framework of the old Reggeon Field Theory. The complete set of cut non-loop enhanced graphs is obtained. Important cancellations between contributions of certain sub-classes of cut diagrams are observed.

1 Introduction

Even nowadays, forty years after the Reggeon Field Theory (RFT) [1] has been proposed, it attracts attention of researches. This is partly due to the fact that a number of important results of the old RFT remain also valid in the perturbative BFKL pomeron calculus [2]. Thus, RFT remains a testing laboratory for novel approaches, prior to their realization within more complicated BFKL framework. On the other hand, a perturbative treatment of peripheral hadronic collisions still remains a challenge, the processes being dominated by “soft” parton physics. Hence, numerous Monte Carlo (MC) generators employ pomeron phenomenology [3] to describe the structure of “underlying” hadronic events, which proved to be a successful approach (see, e.g., [4]).

Yet one usually restricts himself with the comparatively simple quasi-eikonal scheme, where hadron-hadron scattering amplitude is described by diagrams of Fig. 1, corresponding to inde-

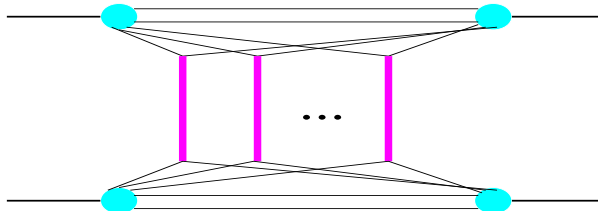


Figure 1: General contribution to hadron-hadron scattering amplitude from multiple pomeron exchanges (vertical thick lines).

pendent pomeron exchanges between the two hadrons¹, and can be expressed via the so-called pomeron quasi-eikonal $\frac{P}{ad}$ as [3]

$$if_{ad}(s;b) = \frac{1}{C_a C_d} e^{\frac{P}{ad}(Y;b)} \frac{i}{1}; \quad (1)$$

with $Y = \ln s$, s and b being c.m. energy squared and impact parameter; C_a - the shower enhancement coefficient. A small imaginary part of $\frac{P}{ad}$ can be neglected in the high energy limit.

¹Here we neglect energy-momentum correlations between multiple re-scatterings [5].

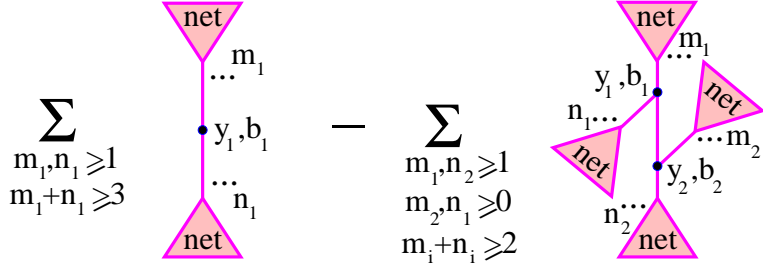


Figure 2: Contribution of non-loop enhanced diagrams to elastic scattering amplitude; the vertices $(y_i; b_i)$ are coupled to m_i projectile and n_i target “net fans”, $i = 1; 2$.

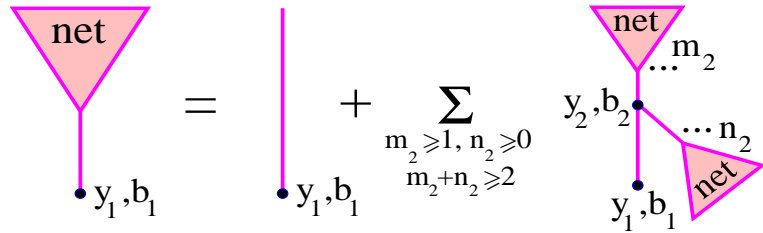


Figure 3: Recursive equation for the “net fan” contribution $\frac{\text{net}}{a \cdot d}(y_1; b_1; \mathcal{Y}; \mathcal{B})$.

However, at high energies one has to account for the contributions of enhanced pomeron diagrams, corresponding to pomeron-pomeron interactions [6]. Thus, in addition to simple pomeron exchanges of Fig. 1, one has to consider multiple exchanges of coupled enhanced graphs. The elastic scattering amplitude can still be written in the usual quasi-eikonal form

$$if_{ad}(s; b) = \frac{1}{C_a C_d} e^{\frac{h}{a \cdot d}(Y; b)} e^{\frac{h}{a \cdot d}(Y; b)} \frac{i}{1}; \quad (2)$$

where for the contribution of coupled enhanced graphs $\frac{\text{enh}}{a \cdot d}$ one obtains the representation² of Fig. 2 [7]. Assuming γ -meson dominance of multi-pomeron vertices this gives

$$\begin{aligned} \frac{\text{enh}}{a \cdot d}(Y; b) = & \frac{G}{C^2} \int_0^Z dy_1 \int_0^Z d^2 b_1 (1 - e^{\frac{\text{net}}{a \cdot d}(1)}) (1 - e^{\frac{\text{net}}{d \cdot a}(1)}) \frac{\text{net}}{a \cdot d}(1) \frac{\text{net}}{d \cdot a}(1) \\ & \frac{G}{C^2} \int_0^Z dy_2 \int_0^Z d^2 b_2 (1 - e^{\frac{\text{net}}{a \cdot d}(1)}) e^{\frac{\text{net}}{d \cdot a}(1)} \frac{\text{net}}{a \cdot d}(1) \\ & (1 - e^{\frac{\text{net}}{d \cdot a}(2)}) e^{\frac{\text{net}}{a \cdot d}(2)} \frac{\text{net}}{d \cdot a}(2); \end{aligned} \quad (3)$$

where G is related to the triple-pomeron coupling r_{3P} as $G = r_{3P} = C^{-3}$, and we used the abbreviations $\frac{\text{net}}{a \cdot d}(i) = \frac{\text{net}}{a \cdot d}(Y - y_i; b_i; \mathcal{Y}; \mathcal{B})$, $\frac{\text{net}}{d \cdot a}(i) = \frac{\text{net}}{d \cdot a}(y_i; b_i; \mathcal{Y}; \mathcal{B})$, $i = 1; 2$. The contribution $\frac{\text{net}}{a \cdot d}(y_1; b_1; \mathcal{Y}; \mathcal{B})$ corresponds to pomeron “nets”, exchanged between hadrons a and d , which are generated starting from a given vertex $(y_1; b_1)$ (y_1, b_1 are rapidity and impact parameter distances between hadron a and this vertex) according to the recursive equation of Fig. 3:

$$\begin{aligned} \frac{\text{net}}{a \cdot d}(y_1; b_1; \mathcal{Y}; \mathcal{B}) = & \frac{p}{a}(y_1; b_1) + \frac{G}{C^2} \int_0^Z dy_2 \int_0^Z d^2 b_2 (1 - e^{\frac{\text{net}}{a \cdot d}(y_2; b_2; \mathcal{Y}; \mathcal{B})}) \frac{\text{net}}{a \cdot d}(y_2; b_2; \mathcal{Y}; \mathcal{B}) \\ & (1 - e^{\frac{\text{net}}{a \cdot d}(y_2; b_2; \mathcal{Y}; \mathcal{B})}) e^{\frac{\text{net}}{d \cdot a}(y_2; b_2; \mathcal{Y}; \mathcal{B})} \frac{\text{net}}{a \cdot d}(y_2; b_2; \mathcal{Y}; \mathcal{B}); \end{aligned} \quad (4)$$

²The representation of Fig. 2 takes into account arbitrary coupled “nets” of pomerons and neglects sub-dominant contributions of “loop” graphs, where some vertices are connected to each other by two or more pomerons [7]. The approach can be generalized to include simplest loop contributions, corresponding to multiple pomeron exchanges between neighboring vertices.

In contrast to the usual “fan” diagram equation (which can be obtained setting $n_2 = 0$ in Fig. 3), the “net fan” contribution ${}_{a,jd}^{\text{net}}$ accounts for absorptive corrections due to re-scatterings both on the projectile and on the target hadrons. The pomeron connected to the initial vertex $(y_1; \mathfrak{b}_1)$ in Fig. 3 will be referred as the “fan handle”.

The knowledge of the elastic scattering amplitude allows one to calculate total and elastic cross sections. However, to obtain partial weights of particular inelastic final states, one has to study unitarity cuts of elastic scattering diagrams and to re-sum the corresponding contributions to all orders. In the following, we shall apply the AGK cutting rules [8] to “net fan” graphs of Fig. 3. Collecting contributions of cuts of certain topologies, we shall use them as building blocks to obtain the complete set of cut diagrams, corresponding to the full discontinuity of the graphs of Fig. 2.

2 Unitarity cuts of “net fans”

It is convenient to separate different unitarity cuts of “net fan” graphs in two classes: in the first sub-set cut pomerons form “fan”-like structures, some examples shown in Fig. 4 (a), (b); in the

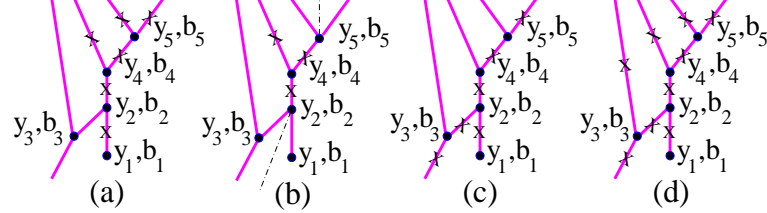


Figure 4: Examples of graphs obtained by cutting the same projectile “net fan” diagram: in the graphs (a) and (b) we have a “fan”-like structure of cut pomerons (marked by crosses); in the diagrams (c) and (d) the cut pomeron, exchanged between the vertices $(y_2; \mathfrak{b}_2)$ and $(y_3; \mathfrak{b}_3)$, is arranged in a “zigzag” way with respect to the “fan handle”. The cut plane is indicated by dot-dashed lines.

diagrams of the second kind some *cut* pomerons are connected to each other in a “zigzag” way, such that pomeron end rapidities are arranged as $y_1 > y_2 < y_3 > \dots$; see Fig. 4 (c), (d).

Let us consider the first class and obtain separately both the total contribution of “fan”-like cuts $2 {}_{a,jd}^{\text{fan}}$ and the part of it, formed by diagrams with the “handle” of the “fan” being uncut, an example shown in Fig. 4 (b), $2 {}_{a,jd}^{\text{fan}}$. Applying AGK cutting rules to the graphs of Fig. 3 and collecting contributions of cuts of desirable structures we obtain for $2 {}_{a,jd}^{\text{fan}}$, $2 {}_{a,jd}^{\text{fan}}$, $2 {}_{a,jd}^{\text{fan}}$ the representations of Figs. 5 and 6, which gives

$$2 {}_{a,jd}^{\text{fan}}(y_1; \mathfrak{b}_1 \mathfrak{Y}; \mathfrak{b}) = 2 {}_{a,jd}^{\text{fan}}(y_1; \mathfrak{b}_1 \mathfrak{Y}; \mathfrak{b}) = 2 {}_{a,jd}^{\text{fan}}(y_1; \mathfrak{b}_1) + \frac{G}{C^2} \int_0^Z dy_2 d^2 b_2 {}_{a,jd}^{\text{fan}}(y_1; \mathfrak{b}_1; y_2; \mathfrak{b}_2) {}_{a,jd}^{\text{fan}}(y_2; \mathfrak{b}_2; y_3; \mathfrak{b}_3) \dots + (1 e^{\text{net}} {}_{a,jd}^{\text{fan}}(y_1; \mathfrak{b}_1; y_2; \mathfrak{b}_2; \dots) {}_{a,jd}^{\text{fan}}(y_2; \mathfrak{b}_2; y_3; \mathfrak{b}_3; \dots) + (1 e^{\text{net}} {}_{a,jd}^{\text{fan}}(y_1; \mathfrak{b}_1; y_2; \mathfrak{b}_2; \dots) {}_{a,jd}^{\text{fan}}(y_2; \mathfrak{b}_2; y_3; \mathfrak{b}_3; \dots) \dots) \quad (5)$$

$$2 {}_{a,jd}^{\text{fan}}(y_1; \mathfrak{b}_1 \mathfrak{Y}; \mathfrak{b}) = \frac{G}{C^2} \int_0^Z dy_2 d^2 b_2 {}_{a,jd}^{\text{fan}}(y_1; \mathfrak{b}_1; y_2; \mathfrak{b}_2) (1 e^{\text{net}} {}_{a,jd}^{\text{fan}}(y_2; \mathfrak{b}_2; y_3; \mathfrak{b}_3; \dots) {}_{a,jd}^{\text{fan}}(y_2; \mathfrak{b}_2; y_3; \mathfrak{b}_3; \dots) + (1 e^{\text{net}} {}_{a,jd}^{\text{fan}}(y_1; \mathfrak{b}_1; y_2; \mathfrak{b}_2; \dots) {}_{a,jd}^{\text{fan}}(y_2; \mathfrak{b}_2; y_3; \mathfrak{b}_3; \dots) + 2 {}_{a,jd}^{\text{fan}}(y_1; \mathfrak{b}_1; y_2; \mathfrak{b}_2; \dots) {}_{a,jd}^{\text{fan}}(y_2; \mathfrak{b}_2; y_3; \mathfrak{b}_3; \dots) \dots) \quad (6)$$

Here the omitted arguments of the eikonal in the integrands in (5-6) read ${}^P = {}^P(y_1, y_2; \mathfrak{b}_1 \mathfrak{b}_2 \mathfrak{Y})$, $X_{a,jd} = X_{a,jd}(y_2; \mathfrak{b}_2 \mathfrak{Y}; \mathfrak{b})$, $X_{d,jd} = X_{d,jd}(y_2; \mathfrak{b}_2 \mathfrak{Y}; \mathfrak{b})$, $X = {}^{\text{net}}; {}^{\text{fan}}; {}^{\text{fan}}; {}^{\text{fan}}$.

The first diagram in the r.h.s. of Fig. 5 is obtained by cutting the single pomeron exchanged between hadron a and the vertex $(y_1; \mathfrak{b}_1)$ in the r.h.s. of Fig. 3, whereas the other ones come from

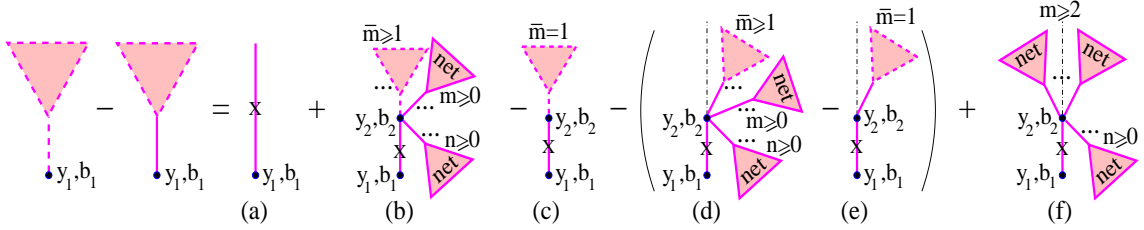


Figure 5: Recursive equation for the contribution $2 \frac{\text{fan}}{a \text{ jd}} - 2 \sim \frac{\text{fan}}{a \text{ jd}}$ of “fan”-like cuts of “net fan” diagrams, the “handle” of the “fan” being cut.

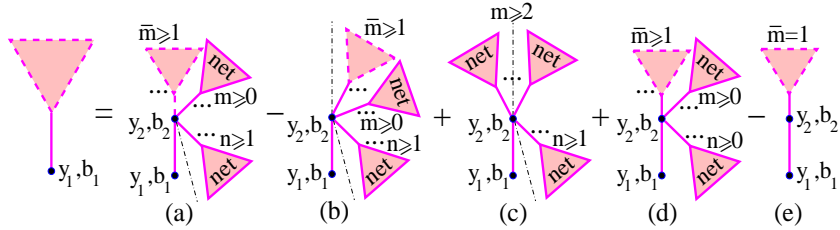


Figure 6: Recursive equation for the contribution $2 \sim \frac{\text{fan}}{a \text{ jd}}$ of “fan”-like cuts of “net fan” diagrams, the “handle” of the “fan” being uncut.

cutting the 2nd graph in the r.h.s. of Fig. 3 in such a way that all cut pomerons are arranged in a “fan”-like structure and the cut plane passes through the “handle” of the “fan”. In graph (b) the vertex $(y_2; b_2)$ couples together $m = 1$ cut projectile “net fans”, each one characterized by a “fan”-like structure of cuts, and any numbers $m; n = 0$ of uncut projectile and target “net fans”. Here one has to subtract pomeron self-coupling contribution ($m = 1, m = n = 0$) - graph (c), as well as the contributions of graphs (d) and (e), where in all m cut projectile “net fans”, connected to the vertex $(y_2; b_2)$, the “handles” of the “fans” remain uncut and all these “handles” and all the m uncut projectile “net fans” are situated on the same side of the cut plane. Finally, in graph (f) the cut plane passes between $m = 2$ uncut projectile “net fans”, with at least one remained on either side of the cut.

In the recursive representation of Fig. 6 for the contribution $2 \sim \frac{\text{fan}}{a \text{ jd}}$ the graphs (a), (b), (c) in the r.h.s. of the Figure are similar to the diagrams (b), (d), (f) of Fig. 5 correspondingly, with the difference that the “handle” of the “fan” is now uncut. Therefore, there are $n = 1$ uncut target “net fans” connected to the vertex $(y_2; b_2)$ in such a way that at least one of them is positioned on the opposite side of the cut plane with respect to the “handle” pomeron. On the other hand, one has to add graph (d), where the vertex $(y_2; b_2)$ couples together $m = 1$ projectile “net fans”, which are cut in a “fan”-like way and have their “handles” uncut and positioned on the same side of the cut plane, together with any numbers $m = 0$ of projectile and $n = 0$ of target uncut “net fans”, such that the vertex remains uncut. Here one has to subtract the pomeron self-coupling ($m = 1, m = n = 0$) - graph (e).

Adding (6) to (5), we obtain

$$2 \frac{\text{fan}}{a \text{ jd}} (y_1; b_1; \mathcal{Y}; \mathcal{B}) = 2 \frac{p}{a} (y_1; b_1) + \frac{G}{C^2} \int_{y_2}^Z dy_2 \int_{b_2}^Z db_2 \frac{p}{a} \\ (e^{2 \frac{\text{fan}}{a \text{ jd}}} - 1) e^{2 \frac{\text{net}}{a \text{ jd}}} + (1 - e^{2 \frac{\text{net}}{a \text{ jd}}})^2 e^{2 \frac{\text{net}}{a \text{ jd}}} 2 \frac{\text{fan}}{a \text{ jd}}; \quad (7)$$

with the solution (c.f. (4))

$$\frac{\text{fan}}{a \text{ jd}} (y_1; b_1; \mathcal{Y}; \mathcal{B}) = \frac{\text{net}}{a \text{ jd}} (y_1; b_1; \mathcal{Y}; \mathcal{B}); \quad (8)$$

To investigate “zigzag”-like cuts of “net fan” graphs, the examples shown in Fig. 4 (c) and (d), we

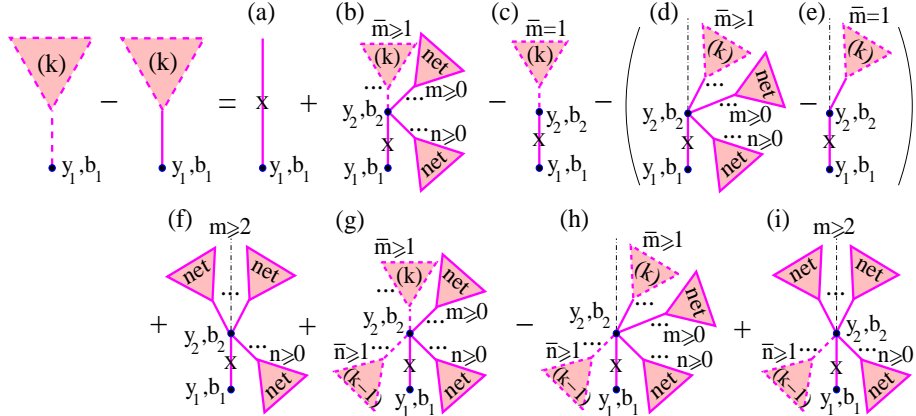


Figure 7: Recursive equation for the cut “net-fan” contribution $2 \frac{\text{net}(k)}{a_{ji}}$ with cut “handle”.

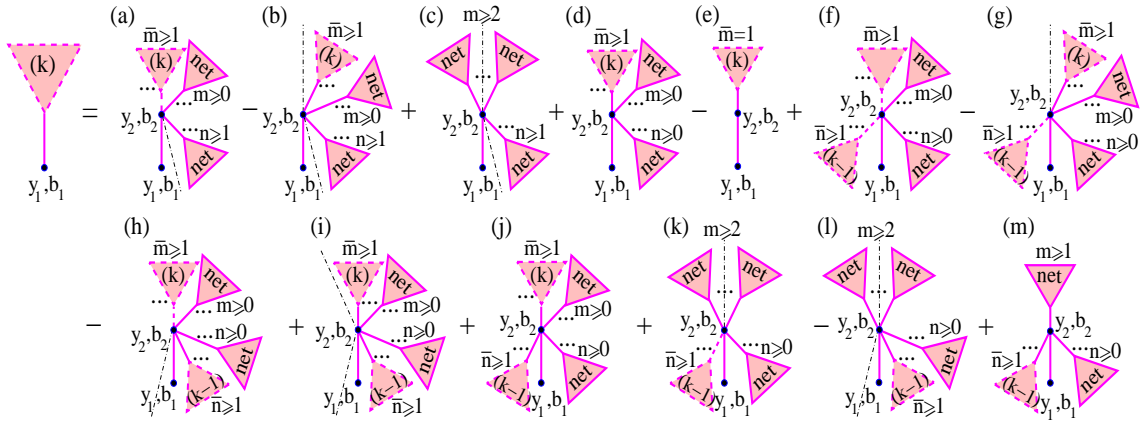


Figure 8: Recursive equation for the cut “net-fan” contribution $2 \frac{\text{net}(k)}{a_{ji}}$ with uncut “handle”.

introduce k -th order cut “net fan” contributions $2 \frac{\text{net}(k)}{a_{ji}}$, which, in addition to the above-considered “fan”-like cut diagrams, contain also ones with up to k cut pomerons connected to each other in a “zigzag” way, i.e., with pomeron end rapidities being arranged as $y_1 > y_2 < \dots > y_{k+1}$. For example, the graphs of Fig. 4 (c) and (d) belong correspondingly to the 2nd and 3rd order cut “net fan” contributions. As before, we consider two subsamples of the diagrams, with the “handles” of the “fans” being cut, $2 \frac{\text{net}(k)}{a_{ji}}$, and uncut, $2 \frac{\text{net}(k)}{a_{ji}}$, which leads us to the recursive equations of Figs. 7 and 8. Compared to the ones of Figs. 5 and 6, they contain additional graphs, Fig. 7 (g)-(i) and Fig. 8 (f)-(m), where the vertex $(y_2; b_2)$ is coupled to $n-1$ cut target “net fans” of $(k-1)$ -th order (we set $\frac{\text{net}(1)}{a_{ji}} = \frac{\text{fan}}{a_{ji}}$, $\frac{\text{net}(1)}{a_{ji}} = \frac{\text{fan}}{a_{ji}}$). Combining the contributions of the graphs of Figs. 7 and 8, we obtain

$$\begin{aligned}
 2 \frac{\text{net}(k)}{a_{ji}}(y_1; b_1; \mathcal{Y}; \mathcal{B}) &= 2 \frac{p}{a}(y_1; b_1) + \frac{G}{C^2} \int_0^Z dy_2 d^2 b_2 \frac{p}{a} \\
 &\quad \left(e^{2 \frac{\text{net}(k)}{a_{ji}}} - 1 \right) e^{2 \frac{\text{net}}{a_{ji}}(1 - e^{\frac{\text{net}}{a_{ji}}})^2} e^{\frac{\text{net}}{d_{ja}}} 2 \frac{\text{net}(k)}{a_{ji}} \\
 &\quad + 2 \frac{h}{(e^{2 \frac{\text{net}(k)}{a_{ji}}} - 1) e^{2 \frac{\text{net}}{a_{ji}}}} + (1 - e^{\frac{\text{net}}{a_{ji}}})^2 2 (1 - e^{\frac{\text{net}}{a_{ji}}}) e^{\frac{\text{net}}{d_{ja}}} (e^{\frac{\text{net}(k)}{d_{ja}}} - 1) \circ ; \quad (9)
 \end{aligned}$$

with the solution

$$\frac{\text{net}(k)}{a_{ji}}(y_1; b_1; \mathcal{Y}; \mathcal{B}) = \frac{\text{net}}{a_{ji}}(y_1; b_1; \mathcal{Y}; \mathcal{B}); \quad (10)$$

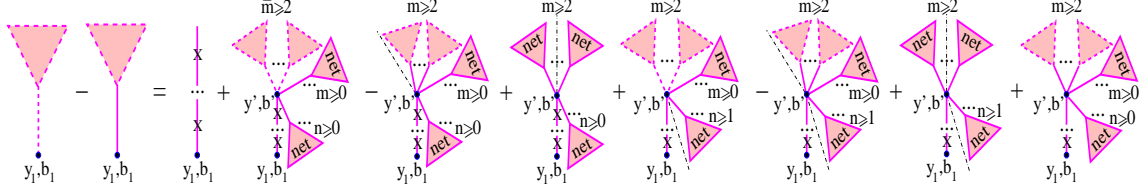


Figure 9: Alternative representation for the “fan”-like cut contribution $2_{a,jd}^{fan} - 2_{a,jd}^{~fan}$ with cut “handle”. Each broken pomeron line denotes a t-channel sequence of pomerons which are separated by vertices connected to uncut projectile and target “net fans”.

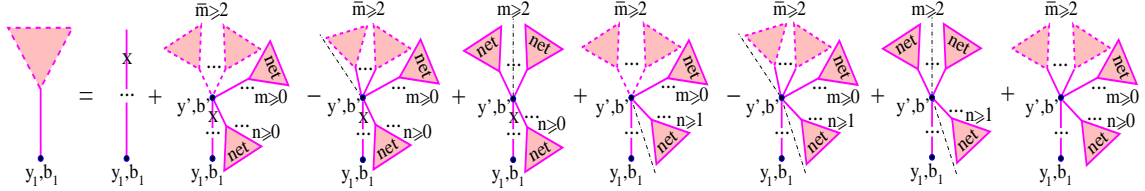


Figure 10: Alternative representation for the “fan”-like cut contribution $2_{a,jd}^{~fan}$ with uncut “handle”. The broken pomeron lines have the same meaning as in Fig. 9.

Thus, for the summary contribution of all cuts of “net fan” graphs of Fig. 2 we obtain $2_{a,jd}^{net}$ $\lim_{k \rightarrow 1} 2_{a,jd}^{net(k)} - 2_{a,jd}^{net}$, as it should be. On the other hand, contributions of various “zigzag” cuts precisely cancel each other

$$2_{a,jd}^{zz(k)} - 2_{a,jd}^{net(k)} - 2_{a,jd}^{net(k-1)} = 0 \quad (11)$$

$$2_{a,jd}^{zz} - 2_{a,jd}^{net} - 2_{a,jd}^{fan} \stackrel{k=2}{=} 2_{a,jd}^{zz(k)} - 0: \quad (12)$$

One can obtain an alternative representation for $\frac{2}{a,jd}^{fan}$, $\frac{2}{a,jd}^{~fan}$, as shown in Figs. 9 and 10, applying (5-6) (correspondingly Figs. 5 and 6) recursively to generate any number of vertices, connected to uncut projectile and target “net fans”, along the “handle” of the “fan”. The broken pomeron lines in Figs. 9 and 10 correspond to t-channel sequences of cut and uncut pomerons which are separated by vertices connected to uncut projectile and target “net fans”. In particular, the contributions $2_{a,jd}^{P_{cc}}$ and $2_{a,jd}^{P_{uc}}$ of the first graph in the r.h.s. of Figs. 9 and 10 correspondingly (the index P_{xy} indicates whether the downmost (uppermost) pomeron in the sequence is cut, $x = c$ ($y = c$), or uncut, $x = u$ ($y = u$)) are defined as (c.f. (5-6))

$$2_{a,jd}^{P_{cc}}(y_1; b_1; \mathcal{Y}; \mathcal{B}) = 2_a^p(y_1; b_1) + \frac{2G}{C^2} \int_0^Z dy_2 d^2 b_2 \stackrel{p}{\mathcal{P}}_i \quad (13)$$

$$(e^{2_{a,jd}^{net} - 2_{a,jd}^{net}} - 1) \left(\frac{P_{cc}}{a,jd} + \frac{P_{uc}}{a,jd} \right) (e^{2_{a,jd}^{net} - 2_{a,jd}^{net}} - 1) \frac{P_{uc}}{a,jd} \quad (13)$$

$$2_{a,jd}^{P_{uc}}(y_1; b_1; \mathcal{Y}; \mathcal{B}) = \frac{2G}{C^2} \int_0^Z dy_2 d^2 b_2 \stackrel{p}{\mathcal{P}}_i \quad (14)$$

$$(1 - e^{2_{a,jd}^{net}}) e^{2_{a,jd}^{net} - 2_{a,jd}^{net}} \left(\frac{P_{cc}}{a,jd} + \frac{P_{uc}}{a,jd} \right) + (e^{2_{a,jd}^{net} - 2_{a,jd}^{net}} - 1) \frac{P_{uc}}{a,jd} : \quad (14)$$

Similarly, we can obtain a recursive representation for k -th order “zigzag”-cut contributions $2_{a,jd}^{zz(k)} - 2_{a,jd}^{net(k)} - 2_{a,jd}^{net(k-1)}$, $2_{a,jd}^{zz(k)} - 2_{a,jd}^{~net(k)} - 2_{a,jd}^{~net(k-1)}$, applying recursively the relations of Figs. 7 and 8 to generate any number of intermediate vertices along the “fan” “handle”, which are connected to uncut and $(k-1)$ -th order cut projectile and target “net fans”, until we end up with the vertex $(y^0; \mathcal{B}^0)$ which either couples together $p = 2$ k -th order projectile “zigzag”-cut

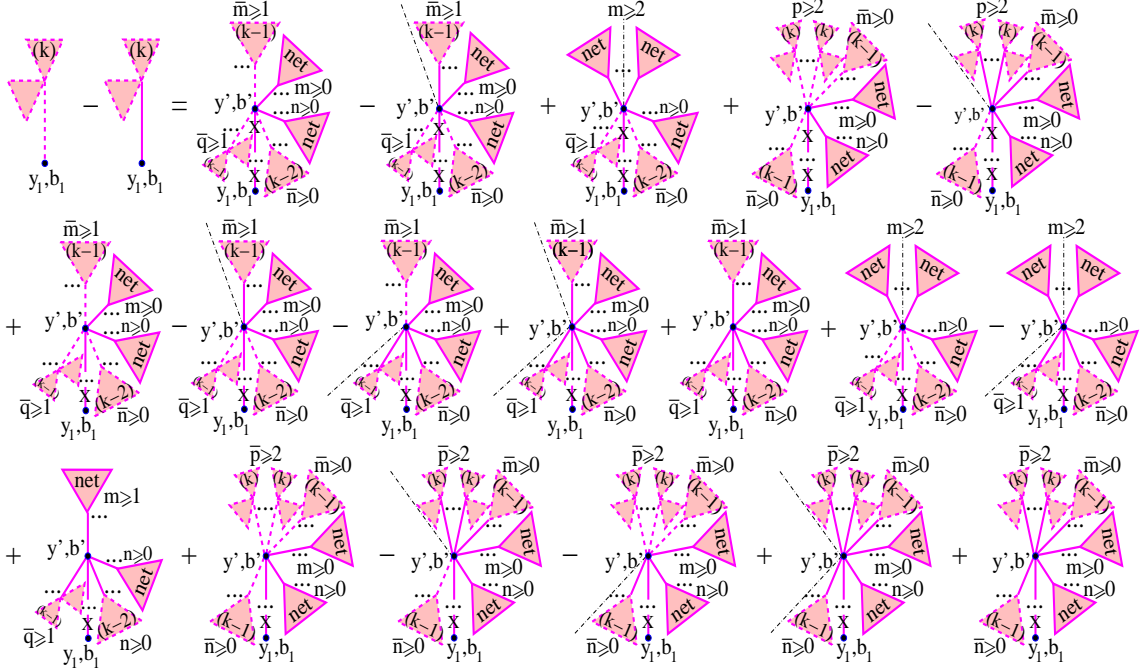


Figure 11: Recursive equation for the contribution $2^{zz(k)}_{a,jl} - 2^{zz(k)}_{a,jl}$ of “zig-zag”-like cuts of “net-fan” diagrams, the “handle” of the “fan” being cut. The broken pomeron line between the vertices $(y_1; b_1)$ and $(y^0; b^0)$ corresponds to a t -channel sequence of cut and uncut pomerons which are separated by vertices connected to uncut and $(k-1)$ -th order cut projectile and target “net fans”.

contributions and any numbers of uncut and $(k-1)$ -th order cut projectile and target “net fans”, or is coupled to $q=1$ $(k-1)$ -th order target “zigzag”-cut contributions (in addition, to any numbers of uncut and $(k-2)$ -th order cut target “net fans”) and to uncut and $(k-1)$ -th order cut projectile “net fans”. The corresponding relation for $2^{zz(k)}_{a,jl} - 2^{zz(k)}_{a,jl}$ is shown in Fig. 11, the one for $2^{zz(k)}_{a,jl}$ looks similarly (c.f. Figs. 9 and 10).

3 Cut enhanced diagrams

We are going to derive the full set of cut diagrams corresponding to s -channel discontinuity of elastic scattering contributions of Fig. 2. Let us start with cut graphs characterized by “tree”-like structure of cut pomerons, which can be constructed coupling any numbers $m; n$ of “fan”-like cut projectile and target “net fans” in one vertex.

First we consider the case of $m; n \in 1$, which leads us to the set of graphs of Fig. 12, where we do not have any double counting of the same contributions. For example, the graphs Fig. 12 (a)-(e) have a single vertex $(y_1; b_1)$, which couples together $m=2$ projectile and $n=2$ target cut “fans”. Correspondingly, different structures of cuts inside the “fans” and different topologies of uncut “fans” result in different diagrams. For the combined contribution of all the graphs of Fig. 12 we obtain, using (8)

$$2^{tree(1)}_{ad}(Y; b) = \frac{2G}{C^2} \int_0^Z dy_1 \int_0^Z db_1 (1 \underset{a,jl}{e} \underset{a,jl}{net} e^{2 \underset{a,jl}{net}}) (1 \underset{d,jl}{e} \underset{d,jl}{net} e^{2 \underset{d,jl}{net}}) + \underset{a,jl}{net} e^{2 \underset{a,jl}{net}} \underset{d,jl}{net} e^{2 \underset{d,jl}{net}} (e^{\underset{d,jl}{fan}} \underset{d,jl}{fan} 1 \underset{a,jl}{\sim fan}) + \underset{d,jl}{net} e^{2 \underset{d,jl}{net}} \underset{a,jl}{net} e^{2 \underset{a,jl}{net}} (e^{\underset{a,jl}{fan}} \underset{a,jl}{fan} 1 \underset{a,jl}{\sim fan}) ; \quad (15)$$

where $X_{a,jl} = X_{a,jl}(Y - y_1; b - b_1; Y; b)$, $X_{d,jl} = X_{d,jl}(y_1; b_1; Y; b)$, $X = \underset{a,jl}{net}, \underset{d,jl}{fan}$.

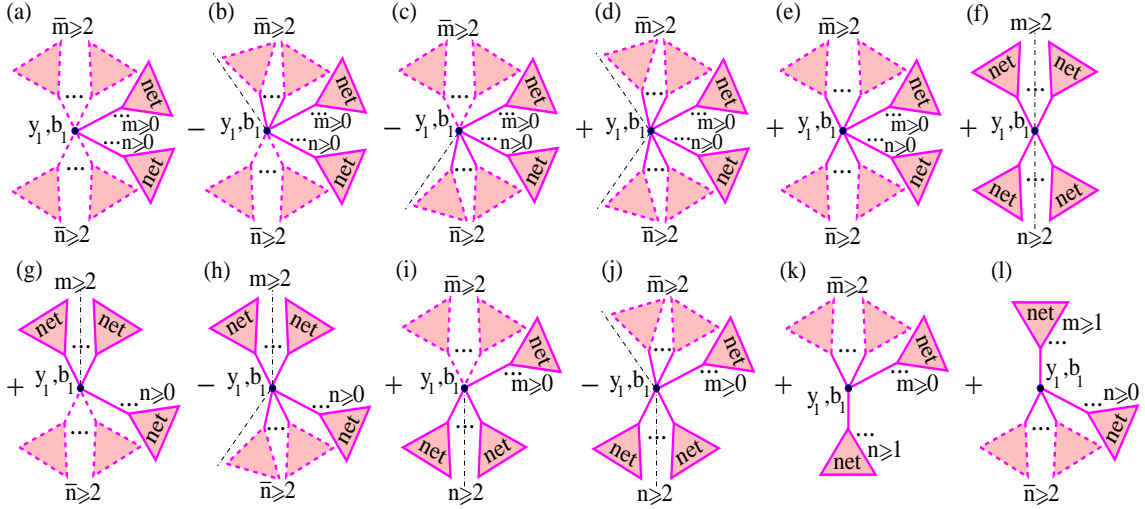


Figure 12: “Tree”-like cut enhanced diagrams. The vertex $(y_1; b_1)$ couples together m projectile and n target “fan”-like cut “net fans”; $m; n \in 1$.

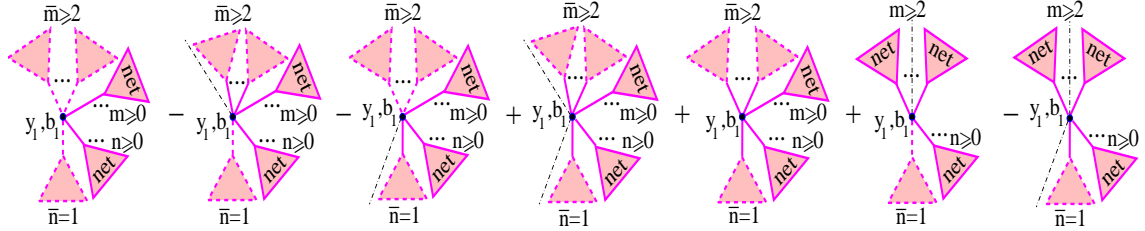


Figure 13: The same as in Fig. 12 for $m \in 1$ and $n = 1$.

Now we come to the case of $m \in 1$ and $n = 1$, which results in the diagrams of Fig. 13. Similarly to the above, we obtain

$$2 \frac{\text{tree}^{(2)}_{\text{ad}}}{\text{ad}} (Y; b) = \frac{2G}{C^2} \int_0^Z dy_1 \int_0^Z db_1 (1 \cdot e^{\frac{\text{net}}{a_{\text{jd}}}} \cdot \text{net} \cdot e^{\frac{2 \cdot \text{net}}{d_{\text{ja}}}}) (\text{net} \cdot e^{\frac{2 \cdot \text{net}}{d_{\text{ja}}}} \cdot \sim_{d_{\text{ja}}}^{\text{fan}} \cdot e^{\frac{\text{net}}{d_{\text{ja}}}}) \circ \text{net} \cdot e^{\frac{\text{net}}{a_{\text{jd}}} \cdot 2 \cdot \frac{\text{net}}{d_{\text{ja}}}} (e^{\sim_{a_{\text{jd}}}^{\text{fan}}} \cdot 1 \cdot \sim_{a_{\text{jd}}}^{\text{fan}}) : \quad (16)$$

Finally we consider the case of $n \in 1$ and $m = 1$, which can be obtained reversing the graphs of Fig. 13 upside-down. There we have to correct for double counting of the same contributions. For example, considering the first diagram of Fig. 13 being reversed upside-down and expanding its projectile cut “fan” using the relations of Figs. 9 and 10, we obtain the set of graphs of Fig. 14. Clearly, the third diagram in the r.h.s. of Fig. 14, being symmetric with respect to the projectile and the target, will appear in a similar expansion of the first graph of Fig. 13. On the other hand, all the other graphs in the r.h.s. of Fig. 14, except the first two, find their duplicates in the expansions of other diagrams of Fig. 13. Thus, the only new contributions are the ones of Fig. 15 (a)-(g). In addition, we have to include the graphs (h)-(j) of the Figure, which correspond to a t -channel sequence of 1–2 cut and uncut pomerons which are separated by vertices connected to uncut projectile and target “net fans”, with the downmost and the uppermost pomerons in the sequence being cut. The contribution of the graphs of Fig. 15 is

$$2 \frac{\text{tree}^{(3)}_{\text{ad}}}{\text{ad}} (Y; b) = \frac{2G}{C^2} \int_0^Z dy_1 \int_0^Z db_1 \left(\frac{P_{cc}}{a_{\text{jd}}} + \frac{P_{uc}}{a_{\text{jd}}} \right) e^{\frac{2 \cdot \text{net}}{a_{\text{jd}}}} \frac{P_{uc}}{a_{\text{jd}}} e^{\frac{\text{net}}{a_{\text{jd}}} \cdot i} (1 \cdot e^{\frac{\text{net}}{d_{\text{ja}}}} \cdot \text{net} \cdot e^{\frac{2 \cdot \text{net}}{d_{\text{ja}}}}) \left(\frac{P_{cc}}{a_{\text{jd}}} + \frac{P_{uc}}{a_{\text{jd}}} \right) (e^{\sim_{d_{\text{ja}}}^{\text{fan}}} \cdot 1 \cdot \sim_{d_{\text{ja}}}^{\text{fan}}) e^{\frac{2 \cdot \text{net}}{a_{\text{jd}}} \cdot \frac{\text{net}}{d_{\text{ja}}}}$$

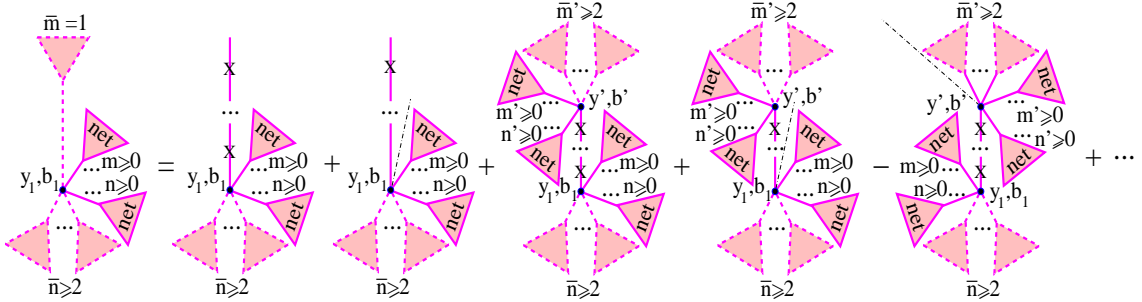


Figure 14: Cut diagram on the l.h.s. can be expanded as shown in the picture.

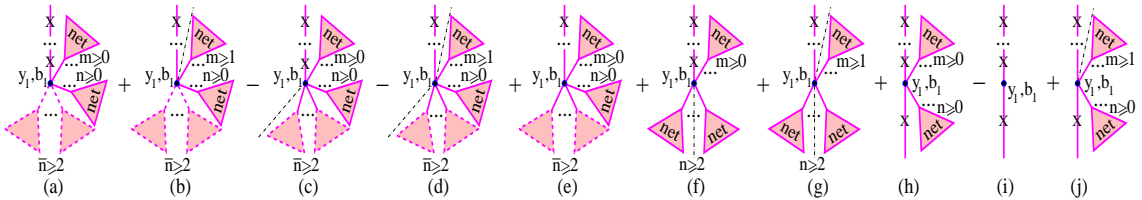


Figure 15: Additional “tree”-like cut diagrams, not included in Figs. 12, 13.

$$+ \frac{h}{p_{cc}} (e^{2 \frac{net}{a_{jjd}} 2 \frac{net}{d_{ja}}} - 1) \frac{p_{uc}}{a_{jjd}} e^{\frac{net}{a_{jjd}} 2 \frac{net}{d_{ja}}} (1 - e^{\frac{net}{a_{jjd}}}) (1 - e^{\frac{net}{d_{ja}}})^i \frac{p}{d}^o : \quad (17)$$

Adding (15-17) together and using (4), (6), (8), (13-14), we can obtain

$$2 \frac{tree}{ad}(Y; b) = \sum_{i=1}^3 2 \frac{tree}{ad}^{(i)}(Y; b) = \frac{2G}{C^2} \int_0^Z dy_1 \frac{Z}{dy_1} \frac{Z}{d^2 b_1} (1 - e^{\frac{net}{a_{jjd}}}) (1 - e^{\frac{net}{d_{ja}}})^i \frac{p}{d}^o (1 - e^{\frac{net}{d_{ja}}})^i \frac{p}{a}^o = 2 \frac{enh}{ad}(Y; b): \quad (18)$$

However, the unitarity requires the sum of all cuts of the diagrams of Fig. 2 to be equal to twice the imaginary part of the elastic scattering contribution, i.e. to $2 \frac{enh}{ad}$. Thus, the contributions of all cuts of non-tree (“zigzag”) type should precisely cancel each other. To verify that, we can construct the complete set of corresponding cut diagrams replacing in Figs. 12 and 13 some contributions $\frac{fan}{a_{jjd}}$ and $\sim \frac{fan}{a_{jjd}}$ ($\frac{fan}{d_{ja}}$ and $\sim \frac{fan}{d_{ja}}$) by $\frac{zz(k)}{a_{jjd}}$ and $\sim \frac{zz(k)}{a_{jjd}}$ ($\frac{zz(k)}{d_{ja}}$ and $\sim \frac{zz(k)}{d_{ja}}$), whereas the others – by $\frac{net(k-1)}{a_{jjd}}$ and $\sim \frac{net(k-1)}{a_{jjd}}$ ($\frac{net(k-1)}{d_{ja}}$ and $\sim \frac{net(k-1)}{d_{ja}}$), starting from $k=2$, etc. Using the representation of Fig. 11 for $2 \frac{zz(k)}{a_{jjd}}$ ($2 \sim \frac{zz(k)}{a_{jjd}}$) to correct for double counts in the same way as above for “tree”-like diagrams, we obtain the set of graphs of Fig. 16. There, the diagrams (a)–(c) contain p 2 k -th order projectile “zigzag”-cut contributions; this gives a factor $(e^{2 \frac{zz(k)}{a_{jjd}}} - 1)^2$, which is equal zero due to (11). Similarly, the graphs (i)–(k) have q 1 k -th order target “zigzag”-cut “fans”, which gives $(e^{2 \frac{zz(k)}{d_{ja}}} - 1) = 0$. The contributions of the graphs (e) and (f) are equal up to a sign and cancel each other; the same applies to the diagrams (m) and (n). Finally, the graphs (d), (g), (h) give together

$$h \frac{G}{C^2} \int_0^Z dy_1 \frac{Z}{dy_1} \frac{Z}{d^2 b_1} (e^{\sim \frac{zz(k)}{a_{jjd}}} - 1) \sim \frac{zz(k)}{a_{jjd}} e^{\sim \frac{net(k-1)}{a_{jjd}}} \frac{net}{a_{jjd}} (e^{2 \frac{net(k)}{d_{ja}}} - 1) e^{\frac{net}{d_{ja}}}^2 + 2 (1 - e^{\frac{net}{d_{ja}}})^i \frac{p}{d}^o ; \quad (19)$$

where the expression in the square brackets vanishes due to (10). Similarly one demonstrates the cancellation for the graphs (l), (o), and (p). This completes the proof of s -channel unitarity of the

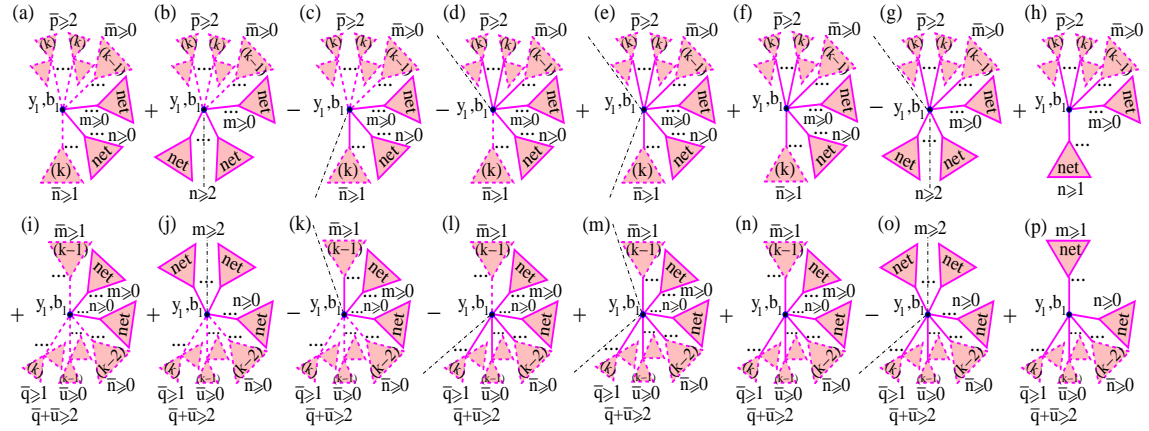


Figure 16: Cut enhanced diagrams with non-“tree” topology of cut pomerons.

approach.³ It is worth stressing that we obtained a cancellation for the contributions of non-“tree” type cut diagrams of Fig. 16 to the total cross section, not to inclusive particle spectra; such graphs have to be taken into consideration in inelastic event generation procedures.

In conclusion, we derived the complete set of cut non-loop enhanced diagrams, as given in Figs. 12, 13, 15, and 16. The obtained results open the way for a consistent implementation of the RFT in hadronic MC models. Details of the corresponding procedure will be discussed elsewhere. On the other hand, as already discussed in [9], the scheme can be applied for calculations of diffraction cross sections and of rapidity gap survival probabilities. It is noteworthy that current analysis does not depend on a particular parameterization for the pomeron exchange amplitude and can be extended for a phenomenological description of “hard” processes [9].

References

- [1] V. N. Gribov, Sov. Phys. JETP **26**, 414 (1968); M. Baker and K. A. Ter-Martirosian, Phys. Rep. **28**, 1 (1976).
- [2] L. V. Gribov, E. M. Levin and M. G. Ryskin, Phys. Rep. **100**, 1 (1983).
- [3] A. B. Kaidalov and K. A. Ter-Martirosyan, Phys. Lett. B **117**, 247 (1982); A. Capella *et al.*, Phys. Rep. **236**, 225 (1994).
- [4] K. Werner, Phys. Rep. **232**, 87 (1993); H. J. Drescher *et al.*, *ibid.* **350**, 93 (2001).
- [5] M. Braun, Sov. J. Nucl. Phys. **52**, 164 (1990); M. Hladik *et al.*, Phys. Rev. Lett. **86**, 3506 (2001).
- [6] O. V. Kancheli, JETP Lett. **18**, 274 (1973); J. L. Cardi, Nucl. Phys. B **75**, 413 (1974); A. Capella, J. Kaplan and J. Tran Thanh Van, *ibid.* **105**, 333 (1976); A. B. Kaidalov, L. A. Ponomarev and K. A. Ter-Martirosyan, Sov. J. Nucl. Phys. **44** (1986) 468.
- [7] S. Ostapchenko, Phys. Lett. B **636**, 40 (2006).
- [8] V. A. Abramovskii, V. N. Gribov and O. V. Kancheli, Sov. J. Nucl. Phys. **18**, 308 (1974).
- [9] S. Ostapchenko, Phys. Rev. D **74**, 014026 (2006).

³Strictly speaking, s -channel unitarity is still violated in certain parts of the kinematic space. For example, one obtains here a negative contribution for double high mass diffraction (central rapidity gap) cross section. The problem is cured when simple “loop” contributions are taken into account; current re-summation method remains applicable in that case too.